



UNIVERSITY OF LEEDS

This is a repository copy of *Whey protein microgel particles as stabilizers of waxy corn starch + locust bean gum water-in-water emulsions*.

White Rose Research Online URL for this paper:
<http://eprints.whiterose.ac.uk/93711/>

Version: Accepted Version

Article:

Murray, BS and Phisarnchananan, N (2016) Whey protein microgel particles as stabilizers of waxy corn starch + locust bean gum water-in-water emulsions. *Food Hydrocolloids*, 56. pp. 161-169. ISSN 0268-005X

<https://doi.org/10.1016/j.foodhyd.2015.11.032>

© 2015, Elsevier. Licensed under the Creative Commons Attribution-NonCommercial-NoDerivatives 4.0 International
<http://creativecommons.org/licenses/by-nc-nd/4.0/>

Reuse

Unless indicated otherwise, fulltext items are protected by copyright with all rights reserved. The copyright exception in section 29 of the Copyright, Designs and Patents Act 1988 allows the making of a single copy solely for the purpose of non-commercial research or private study within the limits of fair dealing. The publisher or other rights-holder may allow further reproduction and re-use of this version - refer to the White Rose Research Online record for this item. Where records identify the publisher as the copyright holder, users can verify any specific terms of use on the publisher's website.

Takedown

If you consider content in White Rose Research Online to be in breach of UK law, please notify us by emailing eprints@whiterose.ac.uk including the URL of the record and the reason for the withdrawal request.



eprints@whiterose.ac.uk
<https://eprints.whiterose.ac.uk/>

1 **Whey protein microgel particles as stabilizers of waxy**
2 **corn starch + locust bean gum water-in-water emulsions**

3

4 Brent S. Murray* and Nataricha Phisarnchananan

5 Food Colloids Group, School of Food Science and Nutrition, University of Leeds, Leeds, LS2 9JT, UK

6 b.s.murray@leeds.ac.uk

7 * Author for correspondence

8

9

10

11 Abstract

12 Food-grade whey protein isolate (WPI) microgel particles were investigated as a particle stabilizer of
13 water-in-water (W/W) emulsions. The microgel particles were produced via the novel method of forcing
14 coarse particles of a pre-formed thermally processed WPI protein gel through a jet homogenizer. The
15 Z-average particle size was 149 ± 89 nm but the particles showed a strong tendency for aggregation
16 when the pH was lowered from pH 7 to 4, when zeta potential also switched from -17 to + 12 mV. The
17 viscoelasticity of suspensions of the particles, measured between 1 and 15 vol.% (0.02 and 3 wt.%)
18 increased with concentration and was also higher at pH 4 than pH 7. However, all the suspensions
19 were only weakly shear thinning, suggesting that they did not form very strong networks. The particles
20 were added (at 1 - 15 vol.%) to a model W/W system consisting of waxy corn starch (S) + locust bean
21 gum (LBG) that normally shows phase separation when the components are mixed at 90 °C then
22 cooled to room temperature (22 to 25 °C). At 10 to 15 vol.% particles and pH 4, visual observation
23 showed striking inhibition of phase separation, for a period of up to 1 year. Confocal laser scanning
24 microscopy suggested that under these conditions extensive aggregation of the microparticles occurred
25 within the starch phase but also possibly at the W/W interface between the starch-rich and gum-rich
26 regions, supporting a Pickering-type mechanism as responsible for the enhanced stabilization of the
27 W/W emulsion by the microgel particles.

28

29 Key words: protein microgel, Pickering, phase separation, stabilization

30

31 1 Introduction

32 Food products are complex systems containing many different kinds of ingredients and so
33 mixtures of aqueous biopolymers have been widely studied for many years due to their important role in
34 the food industry (Garnier, Schorsch & Doublier, 1995). Polysaccharides are polydisperse
35 macromolecules that have been extensively used as thickening and texturizing agent. Starch, as the
36 main storage carbohydrate of many plants, is one of the most important and abundant sources of food
37 for humans. In most common starches the percentages of amylose and amylopectin are 20-30% and
38 70-80% respectively, whilst waxy starches consist of almost exclusively amylopectin, a highly
39 branched, high molecular weight ($> 10^6$ Daltons) polymer of glucose. Galactomannan gums, such as
40 locust bean gum (LBG), are also very high molecular weight polymers of monosaccharide sugars but
41 their molecular structure is substantially different from that of amylopectin. Such gums consist of a
42 substituted linear mannan backbone with short galactose side chains. Thus, LBG forms highly
43 entangled, viscous solutions that are highly shear thinning at relatively low concentrations, whilst
44 amylopectin forms very weak gels but is a good thickening agent at relatively high concentrations,
45 where the highly branched swollen polymer molecules start to overlap. The very different
46 conformational structures of the amylopectin and LBG molecules means that they have difficulty
47 forming simple mixtures even at relatively low concentrations and this leads to their phase separation.

48 Albertsson first reported work on the phase separation of aqueous polysaccharides in 1962 and
49 since then there have been numerous studies of the thermodynamic incompatibility of starch and non-
50 starch hydrocolloids (Tolstoguzov, 1986; Alloncle & Doublier, 1991; Kulicke, 1996; Conder-petit, Pfrirter
51 & Escher, 1997; Closs et al., 1999; Tolstoguzov, 2006; Frith, 2010, Murray & Phisarnchananan, 2014).
52 Phase separation of mixtures of these polysaccharides (in the absence of particles) has been shown
53 elsewhere (Achayuthakan & Suphantharika, 2008; Ptaszek et al., 2009; Simonet, Garnier & Doublier,
54 2000) and such mixtures are used in various products and their phase separation is an issue. So study
55 of these systems is of relevance to real products whilst at the same time starch + gum has proved to be
56 a good model system to test ideas of what types of 'surfactants' might be used to stabilize the water-
57 water interface in phase separating aqueous-soluble polymers.

58 Depending on the relative size and volume fraction of the different polysaccharide-rich phases that
59 form, one can consider such systems as dispersions of one water-rich phase within another, i.e., water-
60 in water (W/W) dispersions (emulsions). Frith (2010) discussed how the detailed microstructure of
61 W/W dispersions could be controlled by solution conditions such as pH, salt, temperature, etc. It is
62 important to understand and be able to control these phase phenomena since excessive phase
63 separation may cause unacceptable changes in the appearance or sensory properties of products in
64 which W/W dispersions exist (Semenova & Dickinson 2010; Firoozmand, Murray and Dickinson, 2012).

65 This paper builds on previous findings (Murray & Phisarnchananan, 2014) where the phase diagram of
66 a starch + gum system was established and the rheology of the separate gum and starch phases was
67 measured over a range of concentrations and shear rates/frequencies. In addition, it was
68 demonstrated that sub-micron solid, hard (silica) particles possessing a range of surface
69 hydrophobicity, i.e., non-food grade, were largely able to inhibit phase separation over a period of
70 several weeks. In this current work the aim was to extend the idea of 'Pickering' stabilization of W/W
71 systems to a new class of food-grade particle – submicron protein microgel particles.

72 Pickering emulsions, where solid particles strongly adsorb at the interface between two fluid
73 phases and protect the dispersed phase from coalescing, were largely ignored after their re-discovery
74 by Pickering in 1907 (Chevalier & Bolzinger, 2013). However, in the past decade there has been
75 renewed interest in Pickering stabilization, partly because of the increasingly novel and wide ranging
76 types of nanoparticles and microparticles that are now available. As far as application to foods is
77 concerned, a continuing challenge is to find effective Pickering particles that are acceptable for use in
78 the food industry (Morris, 2011; Dickinson, E. 2012b; Berton-Carabin & Karin Schröen, 2015).
79 The wetting properties of the particles at the interface (i.e., contact angle) is a key parameter in
80 controlling the effectiveness of the particles as stabilizer and much work has focused on inorganic
81 particles (Binks & Lumsdon, 2000; Binks, Rodrigues, & Frith, 2007; Lopetinsky, Masliyah & Xu, 2006;
82 Yi, Yang, Jiang, Liu & Jiang, 2011) with surface chemistry modification (to increase their hydrophobic
83 nature) or latex particles (Binks, Lumsdon, 2001; Dinsmore, Hsu, Nikolaidis, Marquez, Bausch &
84 Weitz, 2002; Paunov, 2003; Firoozmand, Murray & Dickinson, 2009; Du, Glogowski, Emrick, Russell &
85 Dinsmore, 2010) although neither of these are suitable as food-grade ingredients. Particle aggregation
86 to interfaces and its influence on colloidal stabilization has recently been reviewed by Dickinson
87 (2015a)

88 Herzig et al. (2007) showed that phase separation of an oil/water system (lutidine as the oil phase)
89 can be complete arrested by inclusion of 3 vol.% colloidal surface modified silica particles. In an oil-
90 water system the energy barrier (ΔE) to particle displacement from the interface can reach thousands
91 of $k_B T$ (k_B is the Boltzmann constant and T is the absolute temperature) (Binks & Horozov, 2006; de
92 Folter, van Ruijveb and Velikov 2011; Destribats et al. 2014; Murray & Phisarnchananan 2014). ΔE is
93 given by $\Delta E = \pi r^2 \sigma (1 - |\cos \theta|^2)$, where θ = the three phase contact angle, r = the particles
94 radius and σ = the liquid-liquid interfacial tension. In an oil-water system the interfacial tension is
95 usually at least 1 mN m⁻¹, but with W/W polysaccharide+polysaccharide systems can be extremely low
96 (10⁻⁴ – 10⁻⁶ Nm⁻¹, Shum, Varnell & Weitz, 2012) and so the gain in free energy by particles occupying
97 the interface might be expected to be negligible. Nevertheless, Murray and Phisarnchananan (2014)

98 recently showed that silica particles of varying surface hydrophobicities could apparently inhibit the
99 phase separation of W/W systems consisting of waxy corn starch + LBG or guar gum. Furthermore,
100 Nguyen, Nicolai & Benyahia (2013) have used protein aggregates as particles in controlling phase
101 separation of 'semi-polysaccharide' type W/W system of dextran + poly(ethylene oxide). Protein
102 microgel particles (de Folter et al., 2012, Destribats et al., 2014) are just one type of novel food particle
103 that might be exploited via the Pickering mechanism. Others include chitin nanocrystals (Tzoumaki,
104 Moschakis, Kiosseoglou, & Biliaderis, 2011), cellulose microparticles (Wege et al., 2008), soy protein
105 particles (Liu & Tang, 2013), modified starch particles (Timgren, Timgren, Rayner, Sjöo & Dejmek,
106 2011; Murray, 2011; Yusoff & Murray, 2011; Rayner et al., 2012; Tan et al., 2014), flavonoid particles
107 (Luo et al., 2011), solid lipid particles and emulsion droplets (Gupta & Rousseau, 2012; Hanazawa &
108 Murray, 2013, 2014)

109 Although protein microgel particles cannot really be considered as classic hard particle Pickering
110 stabilizers, particles do not have to be rigid in order to act as good stabilizers, as long as they maintain
111 a size and contact angle sufficient to secure their interfacial attachment as proscribed by eq. (1), so that
112 the term 'Mickering' emulsions has been coined by Schmidt et al. (2011) to describe microgel-particle-
113 stabilized emulsions. In addition, there have been a number of advances recently in the production of
114 truly nanoscale protein aggregate particles of well-defined size or shape (Saglam, Venema, van der
115 Linden & de Vries, R., 2014). Many of these methods rely on heating globular proteins in relatively
116 dilute solution and at extremes of pH, particularly whey protein (Schmitt, et al., 2009, 2010; Schmitt &
117 Ravaine, 2013).

118 In the work reported here we have opted for forming a thermally processed globular protein gel
119 under more conventional conditions, but reduced this gel to significantly small nanogel/microgel
120 particles through efficient processing through a jet homogenizer. The particles have been tested
121 subsequently as a Pickering stabilizer of a true W/W polysaccharide system that we have studied
122 previously (Murray & Phisarnchananan, 2014), consisting of a waxy corn starch (S) and locust bean
123 gum (LBG). It is hoped that such particles and this method of preparation may form a more practical
124 way of applying the Pickering mechanism to control the stability of W/W emulsions. Applications of
125 protein microgel particles in general have recently been reviewed by Dickinson (2015b).

126 **2 Materials and Methods**

127 *2.1 Materials*

128 Gelatinized waxy corn starch (S), product code S9679, and locust bean gum (LBG), product
129 code G0753, were purchased from Sigma-Aldrich (Gillingham, UK). All polysaccharide mixtures were

130 made up in a pH 7 phosphate buffer consisting of $0.05 \text{ mol dm}^{-3} \text{ KH}_2\text{PO}_4 + \text{Na}_2\text{HPO}_4 + 0.05 \text{ mol dm}^{-3}$
131 NaCl. Sodium azide (0.02 wt.%) was also added as a bactericide. The pH was adjusted by adding
132 either $1 \text{ mol dm}^{-3} \text{ NaOH}$ or $1 \text{ mol dm}^{-3} \text{ HCl}$. Rhodamine B (product code R-6626) and acridine orange
133 hemi (zinc chloride) salt, (product code 158550) were also obtained from Sigma-Aldrich. Water purified
134 by a Milli-Q apparatus (Millipore, Bedford, UK), with a resistivity not less than $18.2 \text{ M}\Omega \text{ cm}$, was used
135 for the preparation of all solutions. Silicone oil AS4 was from Fluka (Gillingham, UK). Powdered whey
136 protein isolate (WPI) was obtained from Fonterra Limited (Auckland, New Zealand).

137 2.2 *Preparation of WPI microgel particle suspensions.*

138 The WPI powder was dispersed at 15 wt.% WPI in 200 ml phosphate buffer pH 7 (mentioned above)
139 and stirred under mild magnetic stirring overnight for a complete solubilization. The WPI solution was
140 transferred to glass bottle with plastic screwed top and heated in a temperature-controlled water bath at
141 90°C for 30 minutes. It was then cooled down under running water for 15 minute and stored in the
142 refrigerator overnight. The WPI gel was then roughly broken into pieces with a spatula and then the
143 coarse gel fragments were added to the chambers of a jet homogenizer (Burgaud, Dickinson & Nelson,
144 1990) which were then topped up with buffer. The ratio of the volumes in the two chambers used in the
145 jet homogenizer was 45:55. The fragments were then homogenized at 220 bar. The finer gel fragments
146 obtained were poured in to the larger of the chambers whilst the smaller chamber was filled with buffer
147 and the fragments were homogenized again, but a slightly higher pressure of 300 bar. The volume
148 fraction of microgel particles in this suspension was determined by centrifuging a sample of the
149 suspension in a Beckman Avanti J30i centrifuge using a JA-30.50 rotor at 12000 rpm (approx. 17400 g)
150 until the microparticles sedimented to leave a clear upper aqueous phase. This phase was then
151 carefully removed via a pipette to determine its volume. Before the microparticles were characterized or
152 blended with the starch and gum phases after dilution to the appropriate vol.% with buffer, the
153 suspension sonicated in a Vibra-cell (Sonics&Materials, Newtown USA) for 2 min using 40% amplitude
154 pulses every 2 seconds. (The suspensions also had a notable tendency for foaming and any bubbles
155 that formed during their manipulation were removed via suction through a pipette).

156 2.3 *S + LBG water-in-water emulsion preparation*

157 Stock solutions of starch (7 wt.%) were prepared by dispersing the starch powder in the pH 7
158 phosphate buffer, followed by heating in an oil bath at 90°C for 15 minutes with constant stirring, by
159 hand. Stock solutions of gums were prepared by dispersing 2 wt.% LBG in the buffer under the same
160 conditions as for the starch. The LBG solution was then left to cool and centrifuged at 11000 rpm and
161 25°C for 1 h in a high speed Beckman Coulter(J2-HS) centrifuge to remove insoluble materials. These

162 contributed 20 ± 2 wt.% of the original powders. (Panda (2004) has reported that commercial LBG may
163 contain up to 27% impurities). Stock solutions were stored at room temperature before use. The stock
164 solutions were diluted with buffer to the required concentrations based on the soluble part remaining.
165 To prepare mixtures, both stock solutions were heated separately at $90\text{ }^{\circ}\text{C}$ for 5 minutes before
166 blending. Equal volumes of S and LBG phases were blended with up to 10 ml of the WPI microgel
167 particle suspension. Blends were mixed immediately after removal from the oil bath by an Ultra Turrax
168 T25 homogenizer (IKA-Werke GmbH & Co., Staufen Germany) at 24000 rpm for 1 minute, after which
169 the temperature of the samples had fallen to $70 \pm 5\text{ }^{\circ}\text{C}$ For blends including microgel particles, the
170 particles were added to either the gum or starch phase first. In order to reduce the pH to pH 4, 29 μl of
171 0.25 M HCl was added during the blending via the Ultra Turrax. For samples intended for confocal
172 microscopy, Rhodamine B (RB) and acridine orange (AO) were added during blending to stain starch
173 phase and particles respectively.

174 2.4 Particle size distribution and ζ -potential of WPI microgel particles

175 The particle size distributions of the WPI microgel particles were determined by dynamic light
176 scattering at $25\text{ }^{\circ}\text{C}$ using a Zetasizer Nano-ZS (Malvern instruments, Malvern UK) in a PMMA standard
177 disposal cuvette. Particle sizes were measured after diluting samples with phosphate buffer. The
178 refractive index of WPI and the dispersion medium were set at 1.545 (Purwanti, Moerkens, van der
179 Goot & Boom, 2012) and 1.33, respectively. The absorbance of the protein was assumed = 0.001. The
180 Z-average size or cumulant mean was calculated by the autocorrelation function from Zetasizer
181 software.

182 2.5 Bulk rheology

183 Bulk shear rheology of the WPI suspension was measured with a Kinexus Rheometer (Malvern
184 Instruments, Worcestershire UK) using the *rSpace* software to control the rheometer, measure and
185 analyze the results. The temperature was set at $25\text{ }^{\circ}\text{C}$ in every experiment. The cone and plate
186 cartridge (CP2/60:PL65) was used in every sample. After placing the sample between the cone and
187 plate the sample was then left to achieve steady state for 5 minutes. Viscosities were measured over a
188 range of shear rates using the shear rate mode in *rSpace* software. The starting shear rate was 0.1 s^{-1}
189 and the final shear rate 1 s^{-1} the whole range taking 12 minutes in total. In oscillatory mode, the elastic
190 and viscous components G' and G'' were measured at 1% strain, in the range $0.1 - 1\text{ Hz}$, taking 15 min
191 in total for each run. Silicone oil was layered around the edge of the sample to prevent sample
192 evaporation and drying.

193 2.6 *Visual assessment of the W/W emulsion stability*

194 Freshly emulsions were prepared in 75 x 25 mm flat bottom test tubes sealed with plastic cap,
195 stored at room temperature (22 to 25 °C) and photographed periodically.

196 2.7 *Confocal laser scanning microscopy (CLSM)*

197 CLSM of blends was performed using a Leica TCS SP2 confocal laser scanning microscope
198 (Leica Microsystems, Manheim Germany) connected with a Leica Model DM RXE microscope base.
199 The confocal was used with Ar/ArKr (488, 514 nm) and He/Ne (543, 633 nm) laser sources. Laser
200 excitation of the fluorescent samples was at 514 nm (\approx 29% intensity of laser) for Rhodamine Blue(RB)
201 and 488 nm (\approx 49% intensity of laser) for Acridine Orange(AO). A 20x objective with numerical
202 aperture 0.5 was used to obtain all images, at 1024 x 1024 pixel resolution. 0.5 wt.% of RB and 0.5
203 wt.% AO were dissolved with Millipore water and the solutions were stored in the dark when not being
204 used. For mixtures without WPI particles, 30 μ l of the RB solution were added per 5 ml of the starch
205 solution before blending with LBG. For polysaccharide mixtures with WPI particles, 30 μ l of the AO
206 solution were added per 5 ml of gum phase before blending. After blending the mixtures via the Ultra
207 Turrax, samples without added microgel particles were immediately poured into a well slide 30 mm
208 diameter and 0.3 mm in depth. RB showed preferential staining of the starch whilst the cationic AO
209 showed strong affinity for the WPI microgel particles. Unlabeled areas were therefore assumed to be
210 gum-rich regions. The first image was captured 5 minutes after blending the mixtures. For systems
211 containing microgel particles it was necessary to wait for 20 min for bubbles to rise out of the samples
212 before they could be poured into the well slide and the cover slip added. The appearance of
213 samples was recorded 0.5 to 24 h after blending. Image analysis was performed using Image J
214 software.

215 **3 Results and discussions**

216 3.1 *Microparticle characterization*

217 The heat-induced WPI gel was broken down into very small fragments by its processing through
218 the jet-homogenizer. The dashed line in Fig. 1 illustrates the size distribution of the microgel particles at
219 pH 7. It can be seen that the smallest dimension in the distribution is ca. 250 nm and the largest is
220 about 5 μ m. This upper limit was assumed to be aggregates of particles, since Fig. 1 also shows that
221 after sonication for 2 min the distribution was significantly shifted to lower particles sizes: almost no
222 particles were above 1 μ m, the Z-average size = 149 nm and the distribution showed a significant tail
223 into the sub-100 nm region. Nevertheless, we resist the temptation to refer to these as 'nanoparticles'.

224 Fig. 2(a) shows a confocal micrograph of a 5 wt.% suspension of sonicated WPI microgel particles at
 225 pH 7, stained with Acridine Orange to highlight protein regions (that appear bright in the images). Not
 226 surprisingly, very few particles are visible, given that the above size distribution indicates that most of
 227 the particle would be below the resolution on the microscope system used (ca. 0.4 μm) and/or
 228 Brownian motion would blur their outlines anyway. Fig. 2(b) illustrates micrographs of the same
 229 particles after acidification to pH 4. The formation of large particle aggregates at pH 4 is evident and for
 230 this reason it was not possible to obtain good quality particle size distribution data at pH 4 via the
 231 Zetasizer (the upper range that the Zetasizer can measure is 6 μm). It was possible, however, to
 232 measure the electrophoretic mobility of the WPI particles in dilute suspension. The values obtained
 233 were -1.34 and +0.93 at pH 7 and 4, respectively. Assuming a particle size of 150 nm, these mobility
 234 values convert, via the Smoluchowski assumption, to corresponding zeta potential values of -17.1 and
 235 + 7.4 mV at pH 7 and 4, respectively. WPI mainly consists of β -lactoglobulin and α -lactalbumin and the
 236 isoelectric point (pI) of these two proteins is in the pH range 4.8 to 5.3 (Fox & McSweeney, 2003) so
 237 that charge reversal between pH 7 and 4 was expected. The absolute magnitude of the zeta potential is
 238 seen to be lower at pH 4 than at pH 7 and so this passage through zero net charge on acidification
 239 probably accounts for the greater preponderance of microgel aggregates at the lower pH.

240 3.2 Bulk rheology of WPI microgel particles

241 The intention was to use the WPI microgel particles to try and impart interfacial stability to the
 242 phase-separating regions. Therefore, it was also important to establish if the microgels had any
 243 significant influence on the rheology of the 'bulk' biopolymer phases. If the microgels caused significant
 244 increase in viscosity or gelation of either the starch-rich or gum-rich phases this would also tend to
 245 curtail phase separation. The bulk shear viscosity (η) of 1 - 15 vol.% suspensions of the microgel
 246 particles was measured at 25 °C over the shear rate ($d\gamma/dt$) range 0.1 to 1 s^{-1} . The results are shown in
 247 shown in Figs. 3 (a) and (b), for pH 7 and 4, respectively. All the WPI microgel dispersions exhibited
 248 shear-thinning behavior to some extent, except the 1 vol.% dispersion at pH 7, which within
 249 experimental error was practically Newtonian. For the rest of the samples η was adequately fitted by
 250 the power law model, i.e.,

$$251 \quad \eta = K \left(\frac{d\gamma}{dt} \right)^{n-1} \quad (1)$$

252 The fitting parameters are shown in Table 1 and the curves on Fig. 3 are the fitted power law
 253 behaviour. Two observations are relevant. Firstly, that η was higher at pH 4 than at pH 7 at all
 254 corresponding vol.% particles, reflecting the greater aggregation of the particles at pH 4. Secondly,
 255 none of the samples were strongly shear thinning. This indicates that strong, extensive networks of

256 particles were not formed, nor was the volume fraction of the particles such that they were close
 257 packing even at the highest concentration added, i.e., 15 vol.%. The latter also indicates that the
 258 particles and aggregates below the resolution of the CLSM probably did not have a high aspect ratio.
 259 In any case microgel particles are generally accepted as being quite compressible and the maximum
 260 packing fractions that can be reached are generally much higher than for model hard spheres (Stokes,
 261 2011). Strongly shear thinning behavior is indicated by much lower magnitude of the flow behavior
 262 index n , or typically a good fit to the empirical Cross equation:

$$263 \frac{\eta - \eta_{\infty}}{\eta_0 - \eta_{\infty}} = \frac{1}{1 + K\dot{\gamma}^m} \quad (2)$$

264 : where η_{∞} and η_0 are the limiting high and 'zero' shear rate limiting viscosities. Flocculated particle
 265 networks or solutions of entangled or weakly cross-linked polymers typically follow the Cross equation.
 266 We attempted to fit the data in Fig. 3 to eq. (2) but no convergence was obtained except for the highest
 267 viscosity case, i.e., 15 vol.% at pH 4 (which was also by far the most shear thinning at $n = -0.27$).
 268 However, the value of η_0 required to give a good fit was of the order of 10^{10} Pa s, which seems
 269 physically unrealistic given the range of the experimentally measured viscosity data.

270 Therefore, when the microgel particles were added to either the starch or LBG phase before the
 271 two polymer phases were blended, one might expect some increase in the viscosity of either phase, but
 272 nothing very significant. It should be noted that η of the starch and LBG phases before blending were
 273 considerably greater than the values measured for the WPI microgel dispersions, e.g., 60 and 42 Pa s
 274 at $d\gamma/dt = 0.1 \text{ s}^{-1}$ for 4 wt.% starch and 0.6 wt.% LBG respectively (Murray & Phisarnchananan, 2014).
 275 Thus, any subsequent effect on the phase separation kinetics of including the microgel particles is
 276 unlikely to be due to enhanced viscosity or gel formation of either phase

277 3.3 Macroscopic observations of the effect of particles of W/W emulsions

278 Two series of mixtures of equal volumes of S + LBG were prepared as described above, in the
 279 presence of different vol.% of WPI microgel particles at pH 4 or 7 and observed at regular time
 280 intervals. Pure mixtures of S + LBG (i.e., without particles) showed macroscopic phase separation
 281 within an hour after mixing and were completely phase separated after 3 days. The mixture formed a
 282 more clear LBG-rich phase at the top and a starch-rich phase at the bottom. Fig. 4 shows the
 283 appearance of all the mixtures after 1, 3 and 7 days. At pH 7 (Fig. 4(a)) the phase separation appeared
 284 to be reduced as the concentration of particles increased, since it was progressively more difficult to
 285 observe a more transparent upper phase – for example after 1 day with 10 vol.% particles and with 15
 286 vol.% after 7 days. A slight difficulty in discerning phase separation in all the samples was that they
 287 also showed increased foam stability as the vol.% particles was increased, so that even after 7 days a

288 thin layer of bubbles was observed at the top of the tubes. Such prolonged foam stability is unusual for
289 whey proteins but protein in the form of particles, in this case gel microparticles, may also produce
290 enhanced stabilization of bubbles (Schmitt, Bovay & Rouvet, 2014).

291 Fig. 3(a) shows that the rheology of a 1 vol.% microparticles suspension at pH 7 is essentially
292 Newtonian and this viscosity (ca. 0.02 Pa s) is much lower than the viscosity of the pure starch or gum
293 phase. Nevertheless, Fig. 4(a) shows that after 1 day this low concentration of particles still inhibits
294 phase separation to some extent. Therefore, this slowing down of the phase separation is unlikely to
295 be due to any significant increase in viscosity of either phase due to presence of this low vol.% of
296 particles. The volume fraction of the upper LBG-rich phase decreased as the vol.% of particles
297 increased but after 7 days the differences between the samples had stabilized and the appearance of
298 the mixtures did not significantly change over an additional of observation period of several months.
299 Fig. 4(b) shows the mixtures at pH 4 and overall every sample was more stable to phase separation at
300 pH 4 than at pH 7, at the same time and vol.% particles. With no particles a thin, very clear upper layer
301 formed within 1 day, suggestive of some syneresis, whilst at 5 and 7.5 vol.% particles the mixtures
302 appeared to form a single turbid layer on top of a very clear water-like phase. At 10 and 15 vol.%
303 particles no phase separation was evident after 1 year and the whole sample was completely turbid,
304 although the pH 4 samples appeared to be more optically dense and they seemed to possess less
305 foam.

306 3.4 *Microscopic observations of the effect of particles of on water-in-water emulsions*

307 Fig. 5(a) shows typical confocal micrographs from the S + LBG system, in this case for 2 wt.%
308 starch + 0.3 wt.% LBG 5±2 min after mixing, in the absence of particles. Such a system shows rapid
309 phase separation via spinodal decomposition, as discussed previously (Murray & Phisarnchananan,
310 2014). In real time the system is quite dynamic with movement and fusion of starch-rich domains
311 (bright areas) and LBG-rich domain (dark areas). Thus, macroscopic phase separation occurs quite
312 readily so that within 24 h (Fig. 5(b)) there were only small brighter 'blobs' of variable size range (< 10
313 µm) visible, which are assumed to represent a small fraction of starch remaining within the bulk LBG
314 phase. Figs. 5(c) and 5(d) show representative images of the same system at pH 7 but containing 5
315 vol.% and 10 vol.% WPI microgel particles, respectively, after 24 h. Compared to without added
316 particles (Fig. 5(b)), Fig. 5(c) shows that 5 vol.% particles seemed to have some effect on the system,
317 since some large starch-rich domains were still visible, although nowhere near as many as just after
318 mixing (e.g., Fig. 5(a)), whilst Fig. 5(d) shows that 10 vol.% particles resulted in considerably more
319 persistence of starch rich domains after 24 h. Furthermore, when the system was acidified to pH 4,
320 Figs. 5(e) and 5(f) show that 5 vol.% and 10 vol.% particles had a dramatic effect on the microstructure

321 of the system - even after 24 h something like a fine spinodal decomposition structure persisted,
322 although elements of this seemed somewhat aggregated.

323 Whether there was any definite accumulation of particles at the water-water interface, effecting a
324 Pickering-type stabilization mechanism, was not clear from these images. However, an additional
325 feature of the images with WPI particles present was a greater propensity for the particles(and/or their
326 aggregates) to reside within the starch-rich domains rather than the gum-rich domains. This was the
327 case regardless of whether the particles were deliberately dispersed in the gum phase or the starch
328 phase before blending the two phase together. The propensity for particles to prefer the one phase over
329 another has been noted before: for silica particles and the same starch in a previous paper (Murray &
330 Phisarnchananan, 2014) but also for different particles in completely different bulk phases (Hanazawa
331 & Murray, 2014; Firoozmand et al., 2009). As yet there is no satisfactory explanation for this effect,
332 although the recent review by Dickinson (2015a) indicates the various types of aggregation processes
333 both in the bulk and at the interface that may be involved.

334 3.5 *Image analysis of phase-separating microdomains*

335 Image analysis of a different series of images was used to try and quantify the effects of pH and
336 particle concentration on the phase separation kinetics of the 2 wt.% S + 0.3 wt.% LBG system. Figs.
337 6(a) and (b) show the extracted characteristic length scale (L) as function of time for 5 and 10 vol.%
338 particles at pH 7 and 4, respectively. " L " indicates the largest dominant dimension in any direction on
339 the image. It was determined from the two-dimensional fast-Fourier transform of the captured
340 micrographs using Image J software. In the absence of particles, L was approximately 60 μm after 5
341 min (the shortest aging time for which it was possible to obtain any images) and after 0.5 h discrete
342 domains were undetectable because separate layers had started to form in the well of the slide. In the
343 presence of 5 or 10 vol.% WPI particles at pH 7 (Fig. 6(a)), the starch microdomain sizes showed
344 similar trends, with the starch blobs growing to $L > 150 \mu\text{m}$ after 0.5 h and continuing to grow to $L > 200$
345 μm after 24 h. Fig. 6(b) shows the significant effect of acidifying to pH 4. There was a significant
346 increase in the stability of the domain size with both 5 and 10 vol.% added WPI particles, with a
347 relatively small increase in L from 35 to 60 μm and 20 to 35 μm , respectively, in the first 24 h.
348 Representative of micrographs of some for the compositions have been included on Fig. 6 to give the
349 reader a better idea of the microstructural differences.

350 The analysis of the microstructure is therefore consistent with the macroscopic observations (Fig.
351 4) and the other microscopic observations (Fig. 5), that increasing concentrations of particles seem to
352 inhibit phase separation of the gum + starch system, especially at pH 4 compared to pH 7.

3.6 Bulk rheology of the starch and gum in the presence of WPI microgel particles

From all the above results, it is clear that WPI microgel particles have the ability to inhibit microscopic domain growth and macroscopic phase separation. It is well known that WPI and whey protein microgel particles can form gel networks in a bulk aqueous phase (Vincent & Saunders, 2011; Schmitt, Bovay & Rouvet, 2014) so it is important to test the effect of adding the WPI particles into each domain, in case the inhibition is simply due to a significant increase in the viscosity of either phase. Therefore, WPI microgel particles were dispersed in the separate bulk LBG and starch phases at the different particle concentrations and the bulk rheology measured. Since the major effects of particle addition were at pH 4, these measurements were only conducted at this pH. Fig. 7 shows the bulk viscosity η at a constant shear rate = 0.1 s^{-1} (Fig. 7(a)) plus the storage modulus (G') and loss modulus (G'') at 0.1 Hz and 1% strain (Figs. 7(b) and (c), respectively). These low shear conditions were selected so as to be as close as possible to the solutions at rest, whilst still obtaining reproducible results.

Fig. 7 clearly shows that up to 10 vol.% WPI microgel particles added to 4 wt.% S, there was no significant increase in η , G' or G'' . In fact, there was a slight decrease in η for particle concentrations below 10 vol.% whilst for 15 vol.% particles η approximately doubled. For G' and G'' the only significant increase also occurred between 10 and 15 vol.%. In contrast, η , G' and G'' remained considerably lower for 0.6 wt.% LBG across the whole range of addition of particles: 0 to 15 vol.%. (Note these two separate concentrations of gum and starch form the same effective final concentrations in the mixtures observed in Figs. 4, 5 and 6 above). Consequently, it seems unlikely that an increase in the viscoelasticity of the gum phase due to the addition of the microgel particles can explain the inhibition of phase separation. It does seem that a significant increase in the viscoelasticity of the starch phase can occur at >10 vol.% microgel particles, probably due to their aggregation in this phase. A likely cause of this might be depletion flocculation of the microgel particles by free polymer (Vincent & Saunders, 2011), in this case the starch molecules. However, since inhibition appears to occur at particle concentrations at and below 10 vol.% particles, plus the fact that the same dynamics occur if the particles are first mixed into the gum phase, an increase in the viscosity of the starch phase due to microgel particle aggregation within this phase similarly cannot explain all the inhibition effects observed. The same conclusion was reached (Murray & Phisarnchananan, 2014) for silica particle addition to the same system, where stabilization by silica particles occurred in particle concentration ranges where no significant increase in bulk phase viscosity occurred due to particle addition.

Detailed measurements of the viscoelasticity of the whole system under going phase separation were not measured, since if phase separation occurs one cannot reproducibly measure and interpret this rheology, since different heights of sample will have different viscoelasticity. However, it is

387 interesting to speculate how the viscoelasticity of the continuous starch phase might hinder the rise of
 388 blobs gum phase within it, or the fall of discontinuous starch blobs within a continuous gum phase. To
 389 this end, we have calculated the theoretical creaming velocity (V_s) of spherical blobs of 0.3 wt.% gum
 390 phase of nominal diameter = 60 μm rising through a continuous starch phase at [S] = 2 wt.%, from
 391 Stokes Law:

$$392 \quad V_s = \frac{d^2 \Delta \rho g}{18 \eta} \quad (3)$$

394
 395 :where $\Delta \rho$ = the density difference between the starch and gum phase, g = acceleration due to gravity,
 396 d = the (gum-rich) blob diameter (assumed spherical) and η = the viscosity of the continuous (starch)
 397 phase. It seems reasonable to suppose that this is slower than starch blobs falling gum phase, since
 398 the measurements of the individual phases showed that η of the S phase + microgel particles was
 399 higher than that of G + particles (see Figure 7). The density of the starch and gum phases were
 400 measured as 1.01 and 0.89 g cm^{-3} , respectively. Using the value of $\eta = 0.51 \text{ Pa s}$, measured at the
 401 lowest shear rate (0.1 s^{-1}) for the system with 10% microgel particles at pH 7, the calculated creaming
 402 velocity is $0.46 \mu\text{m s}^{-1}$. Notwithstanding the fact that creaming probably does not follow Stokes law
 403 exactly, but will be more hindered, this creaming velocity easily predicts gross visible phase separation
 404 in test tubes of the height used (75 mm) since the distance of creaming of such blobs would be 75 mm
 405 in less than 2 days. However, systems such as this have not showed any significant separation over 1
 406 year of storage. Consequently, the growth of the gum-rich domains to sizes even as large as this may
 407 be assumed to be significantly curtailed by the presence of the microgel particles.

408

409 **4 Conclusions**

410 Water-in-water (W/W) emulsions formed by mixing waxy corn starch and locust bean gum solutions
 411 could be stabilized by addition of whey protein isolate (WPI) microgel particles (size ca. 150 nm). The
 412 stability depended upon the concentration of the particles and pH of the system. Stability was
 413 increased with increasing concentration of particles and particularly on lowering the pH from 7 to 4.
 414 The particles aggregated at pH 4 and showed a strong preference for the starch domains rather than
 415 gum phase under all conditions. At pH 4 extensive aggregation of the particles was observed in the
 416 starch phase. However, neither particle aggregation in the starch phase nor any increase in the
 417 viscoelasticity of the gum or starch due to the addition of the particles are able to account for the
 418 inhibition of phase separation. The individual microgel particles were too small to be discerned at the

419 W/W interface via confocal microscopy, but in the absence of other evidence, it seems likely that
420 accumulation and aggregation of the protein particles at the W/W interface could account for the
421 enhanced stability, as proposed by Nyguen, Nicolai & Benyahia (2013) for WPI particles of similar size,
422 probably enhanced by their aggregation at the lower pH. In a similar way, Nguyen, Wang, Saunders,
423 Benyahia & Nicolai (2015) have recently shown how the stability of their dextran+PEO W/W system,
424 when stabilized by synthetic cross-linked polymer microgel particles, can be significantly changed by
425 altering the pH or ionic strength and thus the repulsion between the microgel particles at the W/W
426 interface.

427 **5 References**

- 428 Achayuthakan, P., & Suphantharika, M. (2008). Pasting and rheological properties of waxy corn starch
429 as affected by guar gum and xanthan gum. *Carbohydrate Polymers* 71, 9–17.
- 430 Albertsson, P. (1962). Partition methods for fractionation of cell particles and macromolecules.
431 *Methods of biochemical analysis*.10, pp.229–262.
- 432 Alloncle, M., & Doublier, J. (1991). Viscoelastic properties of maize starch/hydrocolloid pastes and gels.
433 *Food Hydrocolloids*, 5, 455–467.
- 434 Binks, B., & Horozov, T. (2006). Colloidal particles at liquid interfaces: an introduction *In*: B. Binks & T.
435 Horozov, ed. *Colloidal particles at liquid interfaces*. Cambridge: Cambridge University Press, pp. 1–74.
- 436 Binks, B., & Lumsdon, S. (2000). Effects of oil type and aqueous phase composition on oil–water
437 mixtures containing particles of intermediate hydrophobicity. *Physical Chemistry & Chemical Physics*, 2,
438 2959–2967.
- 439 Binks B. P., & Lumsdon S. O. 2001. Pickering emulsions stabilized by monodisperse latex particles:
440 effects of particle size. *Langmuir*, 17, 4540–47.
- 441 Binks, B. P., Rodrigues, J. A., & Frith, W. J. (2007). Synergistic interaction in emulsions stabilized by a
442 mixture of silica nanoparticles and cationic surfactant. *Langmuir*, 23, 3626–3636.
- 443 Berton-Carabin, C. C., & Karin Schröen, K. (2015) Pickering emulsions for food applications:
444 background, trends, and challenges. *Annual Review of Food Science & Technology*, 6, 12.1–12.35
445 doi:10.1146/annurev-food-081114-110822.
- 446 Burgaud, I., Dickinson, E., & Nelson, P. V. (1990). An improved high pressure homogenizer for making
447 fine emulsions on a small scale. *International Journal of Food Science & Technology*, 25, 39–46.
- 448 Cheung Shum, H., Varnell, J., & Weitz, D. A. (2012). Microfluidic fabrication of water-in-water (w/w) jets
449 and emulsions. *Biomicrofluidics*, 6, 12808–12809

- 450 Chevalier, Y., & Bolzinger, M. (2013). Emulsions stabilized with solid nanoparticles: Pickering
451 emulsions. *Colloids & Surfaces A: Physicochemical & Engineering Aspects*, 439, 23–34.
- 452 Closs, C., Conder-Petit, B., Roberts, I., Tolstoguzov, V., & Escher, F. (1999). Phase separation and
453 rheology of aqueous starch/galactomannan systems. *Carbohydrate Polymers*, 39, 67–77.
- 454 Conde-Petit, B., Pfirter, A., & Escher, F. (1997). Influence of xanthan on the rheological properties of
455 aqueous starch-emulsifier systems. *Food Hydrocolloids*, 11, 393–399.
- 456 deFolter, J., van Ruijven, M., & Velikov, K. (2012). Oil-in-water Pickering emulsions stabilized by
457 colloidal particles from the water-insoluble protein zein. *Soft Matter*, 8, 6807–??.
- 458 Destribats, M., Rouvet, M., Gehin-Delval, C., Schmitt, C., & Binks, B. (2014). Emulsions stabilised by
459 whey protein microgel particles: towards food-grade Pickering emulsions. *Soft Matter*, 10, 6941–6954.
- 460 Dickinson, E. (2012a). Stabilising emulsion-based colloidal structures with mixed food ingredients.
461 *Journal of the Science of Food & Agriculture*, 93, 710–721.
- 462 Dickinson, E. (2012b). Use of nanoparticles and microparticles in the formation and stabilization of food
463 emulsions. *Trends in Food Science & Technology*, 24, 4–12.
- 464 Dickinson, E. (2015a). Structuring of colloidal particles at interfaces and the relationship to food
465 emulsion and foam stability. *Journal of Colloid & Interface Science*, 449, 38–45.
- 466 Dickinson E (2015b). Microgels – An alternative colloidal ingredient for stabilization of food
467 emulsions. *Trends in Food Science & Technology*, 43, 178–188.
- 468 Dinsmore, A. D., Hsu, M. F., Nikolaidis, M. G., Marquez, M., Bausch, A. R., & Weitz, D. A. (2002).
469 Colloidosomes: selectively permeable capsules composed of colloidal particles. *Science*, 298, 1006–
470 1009.
- 471 Du, K., Glogowski, E., Emrick, T., Russell, T. P., & Dinsmore, A. D. (2010). Adsorption energy of nano-
472 and microparticles at liquid–liquid interfaces. *Langmuir*, 26, 12518–12522.
- 473 Firoozmand, H., Murray, B., & Dickinson, E. (2009). Interfacial structuring in a phase-separating mixed
474 biopolymer solution containing colloidal particles. *Langmuir*, 25, 1300–1305.
- 475 Firoozmand, H., Murray, B., & Dickinson, E. (2012). Microstructure and elastic modulus of mixed gels of
476 gelatin+oxidized starch: effect of pH. *Food Hydrocolloids*, 26, 286–292.
- 477 Fox, P. F., & McSweeney, P. L. H. (Eds.) (2003) *Advanced Dairy Chemistry: Volume 1: Proteins*,
478 Springer US.
- 479 Frith, W. (2010). Mixed biopolymer aqueous solutions – phase behaviour and rheology. *Advances in*
480 *Colloid & Interface Science*, 161, 48–60.
- 481 Garnier, C., Schorsch, C., & Doublier, J. (1995). Phase separation in dextran/locust bean gum
482 mixtures. *Carbohydrate Polymers*, 28, 313–317.

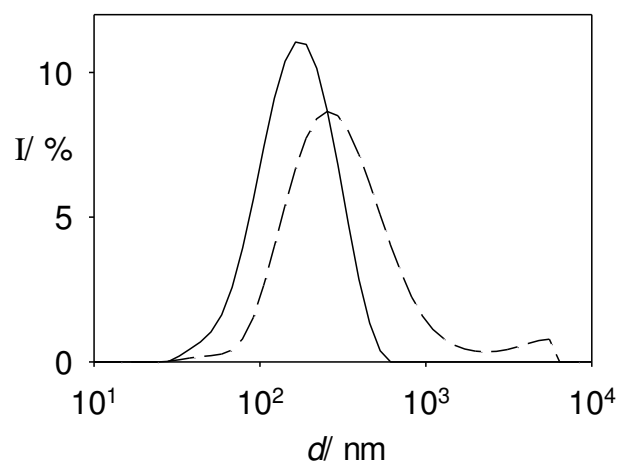
- 483 Gupta, R., & Rousseau, D. (2012). Surface-active solid lipid nanoparticles as Pickering stabilizers for
484 oil-in-water emulsions. *Food & Function*, 3, 302–3011.
- 485 Hanazawa, T., & Murray, B. (2013). Effect of oil droplets and their solid/liquid composition on the phase
486 separation of protein–polysaccharide mixtures. *Langmuir*, 29, 9841–9848.
- 487 Hanazawa, T., & Murray, B. 2014. The influence of oil droplets on the phase separation of protein–
488 polysaccharide mixtures. *Food Hydrocolloids*, 34,128–137.
- 489 Herzig, E., White, K., Schofield, A., Poon, W., & Clegg, P.(2007). Bicontinuous emulsions stabilized
490 solely by colloidal particles. *Nature Materials*, 6, 966–971.
- 491 Kulicke, W., Eidam, D., Kath, F., Kix, M., & Kull, A. (1996). Hydrocolloids and rheology: regulation of
492 visco-elastic characteristics of waxy rice starch in mixtures with galactomannans. *Starch/Stärke*, 48,
493 105–114.
- 494 Liu, F., & Tang, C. (2013). Soy protein nanoparticle aggregates as Pickering stabilizers for oil-in-water
495 emulsions. *Journal of Agricultural & Food Chemistry*, 61, 8888–8898.
- 496 Lopetinsky, R. J. G., Masliyah, J. H., & Xu, Z. (2006). Solids-stabilized emulsions: a review. In B. P.
497 Binks, & T. S. Horozov (Eds.), *Colloidal particles at liquid interfaces* (pp. 186–224). Cambridge:
498 Cambridge University Press.
- 499 Luo, Z., Murray, B., Yusoff, A., Morgan, M., Povey, M., & Day, A. (2011). particle-stabilizing effects of
500 flavonoids at the oil–water interface. *Journal of Agricultural & Food Chemistry*, 59, 2636–2645.
- 501 McClements, D., & Keogh, M. (1995). Physical properties of cold-setting gels formed from heat-
502 denatured whey protein isolate. *Journal of the Science of Food & Agriculture*, 69, 7–14.
- 503 Morris, V. (2011). Emerging roles of engineered nanomaterials in the food industry. *Trends in*
504 *Biotechnology*, 29, 509–516.
- 505 Murray, B. S., & Phisarnchananan, N. (2014). The effect of nanoparticles on the phase separation of
506 waxy corn starch+locust bean gum or guar gum. *Food Hydrocolloids*, 42, 92–99.
- 507 Murray, B. S., Durga, K., Yusoff, A., & Stoyanov, S. (2011). Stabilization of foams and emulsions by
508 mixtures of surface active food-grade particles and proteins. *Food Hydrocolloids*, 25, 627–638.
- 509 Nguyen, B., Nicolai, T., & Benyahia, L. (2013). Stabilization of water-in-water emulsions by addition of
510 protein particles. *Langmuir*, 29, 10658–10664.
- 511 Nguyen, B. T., Wang, W. K., Saunders, B. R., Benyahia, L., & Nicolai, T. (2015). pH-responsive water-
512 in-water Pickering emulsions. *Langmuir*, 31, 3605–3611.
- 513 Panda, H. (2004). *The complete technology book on natural products (forest based)*. Delhi: Asia Pacific
514 Business Press.

- 515 Paunov V. N. (2003). Novel method for determining the three-phase contact angle of colloid particles
516 adsorbed at air-water and oil-water interfaces. *Langmuir*, 19, 7970–7976.
- 517 Ptaszek, A., Berski, W., Ptaszek, P., Witczak, T., Repelewicz, U., & Grzesik, M. (2009). Viscoelastic
518 properties of waxy maize starch and selected non starch hydrocolloids gel. *Carbohydrate Polymer*, 76,
519 567–577.
- 520 Purwanti, N., Moerkens, A., van der Goot, A., & Boom, R. (2012). Reducing the stiffness of
521 concentrated whey protein isolate (WPI) gels by using WPI microparticles. *Food Hydrocolloids*, 26,
522 240–248.
- 523 Rayner, M., Sjö, M., Timgren, A., & Dejmeek, P. (2012). Quinoa starch granules as stabilizing particles
524 for production of Pickering emulsions. *Faraday Discussions*, 158, pp.139-155.
- 525 Saglam, D., Venema, P., van der Linden, E., & de Vries, R. (2014). Design, properties, and
526 applications of protein micro- and nanoparticles. *Current Opinion in Colloid and Interface Science*, 19,
527 428–437.
- 528 Semenova, M., & Dickinson, E. (2010). *Biopolymers in food colloids*. Leiden: Brill.
- 529 Schmidt, S., Liu, T., Rütten, S., Phan, K.-H., Möller, M., & Ritzering, W. (2011). Influence of microgel
530 architecture and oil polarity on stabilization of emulsions by stimuli-sensitive core-shell poly(N-
531 isopropylacrylamide-co-methacrylic acid) microgels: Micking versus Pickering behaviour? *Langmuir*,
532 27, 9801–9806.
- 533 Schmitt, C., Bovay, C., Vuillomenet, A.-M., Rouvet, M., Bovetto, L., Barbar, R., & WSanchez C. (2009).
534 Multiscale characterization of individualized β -lactoglobulin microgels formed upon heat treatment
535 under narrow pH range conditions. *Langmuir*, 25, 7899–7909.
- 536 Schmitt, C., Moitzi, C., Bovay, C., Rouvet, M., Bovetto, L., Donato, L., Leser, M. E., Schurtenberger, P.,
537 & Stradner, A. (2010). Internal structure and colloidal behaviour of covalent whey protein microgels
538 obtained by heat treatment. *Soft Matter*, 6, 4876–4884.
- 539 Schmitt, V., & Ravaine, V. (2013). Surface compaction versus stretching in Pickering emulsions
540 stabilized by microgels. *Current Opinion in Colloid and Interface Science*, 18, 532–541.
- 541 Schmitt, C., Bovay, C., & Rouvet, M. (2014). Bulk self-aggregation drives foam stabilization properties
542 of whey protein microgels. *Food Hydrocolloids*, 42, 139–148
- 543 Simonet, F., Garnier, C., & Doublier, J.L. (2000). Partition of proteins in the aqueous guar/dextran two-
544 phase system. *Carbohydrate Polymer*, 14, 591–600.
- 545 Stokes, J. R. (2011). *Rheology of industrially relevant microgels*. In A. Fernandez Nieves, H. Wyss, J.
546 Mattsson, & D. A. Weitz (Eds.), *Microgel suspensions*. Weinheim: Wiley–VCH, Chap. 13.

- 547 Tan, Y., Xu, K., Niu, C., Liu, C., Li, Y., Wang, P., & Binks, B. P. (2014). Triglyceride–water emulsions
548 stabilised by starch-based nanoparticles. *Food Hydrocolloids*, 36, 70–75.
- 549 Timgren, A., Rayner, M., Sjöo, M., & Dejmeck, P. (2011). Starch particles for food based Pickering
550 emulsions. *Procedia Food Science*, 1, 95–103.
- 551 Tolstoguzov, V. (1986). Functional properties of food macromolecules *In*: J. Mitchell & D. Ledward, ed.
552 London: Elsevier Applied Science, p. 385.
- 553 Tolstoguzov, V. (2006). Phase behavior in mixed polysaccharide systems *In*: M. Alistair et al., ed. *Food*
554 *polysaccharides and their application*. Florida: CRC Press Inc., pp. 589-620.
- 555 Tzoumaki, M., Moschakis, T., Kiosseoglou, V., & Biliaderis, C. (2011). Oil-in-water emulsions stabilized
556 by chitin nanocrystal particles. *Food Hydrocolloids*, 25, 1521-1529.
- 557 Vincent, B., & Saunders, B. R. (2011). Interactions and colloid stability of microgel particles. In A.
558 Fernandez Nieves, H. Wyss, J. Mattsson, & D. A. Weitz (Eds.), *Microgel suspensions*. Weinheim:
559 Wiley–VCH, Chap. 6.,
- 560 Wege, H., Kim, S., Paunov, V., Zhong, Q., & Velev, O. (2008). Long-term stabilization of foams and
561 emulsions with in-situ formed microparticles from hydrophobic cellulose. *Langmuir*, 24, 9245-9253.
- 562 Yi, C. L., Yang, Y. Q., Jiang, J. Q., Liu, X. Y., & Jiang, M. (2011). Research and application of particle
563 emulsifiers. *Progress in Chemistry*, 23, 65–79.
- 564 Yusoff, A., & Murray, B. S. (2011). Modified starch granules as particle-stabilizers of oil-in-water
565 emulsions. *Food Hydrocolloids*, 25, 42–55.
- 566

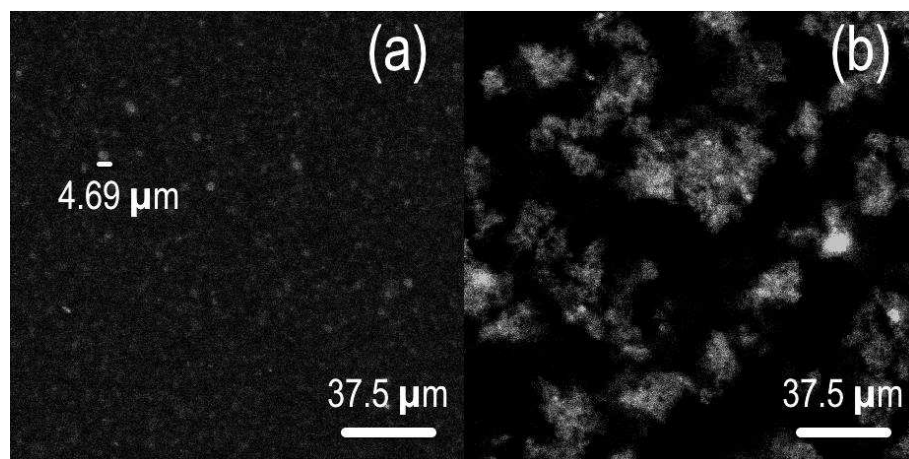
567 Figure 1

568



569

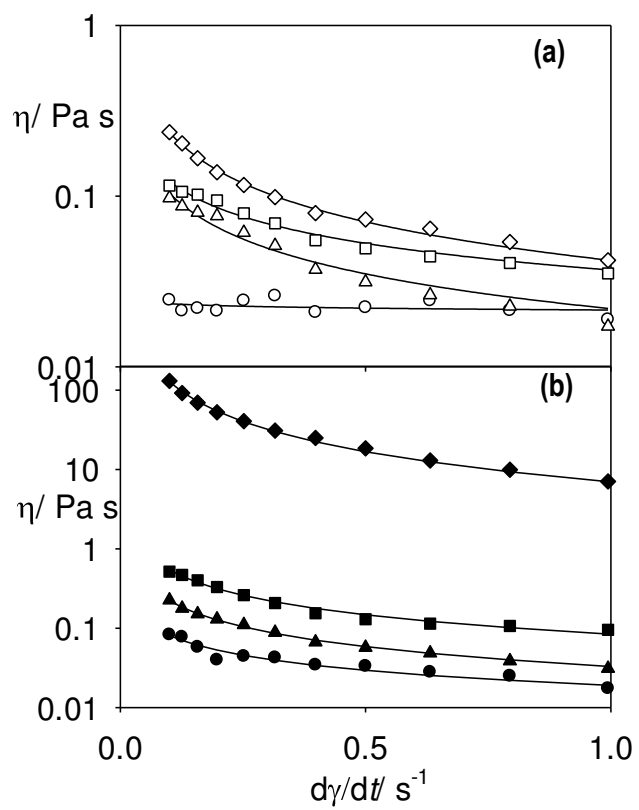
570 Figure 2



571

572

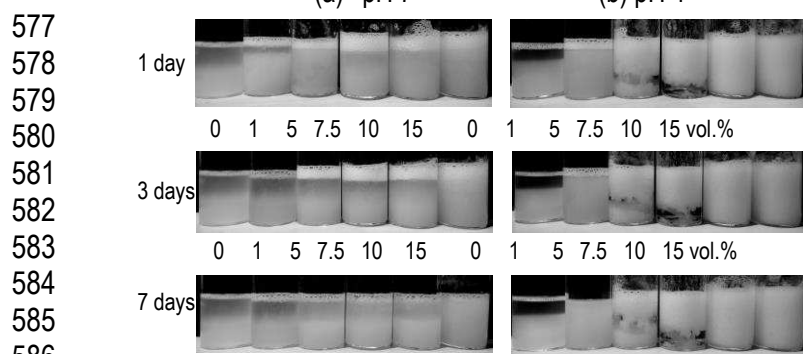
573 Figure 3



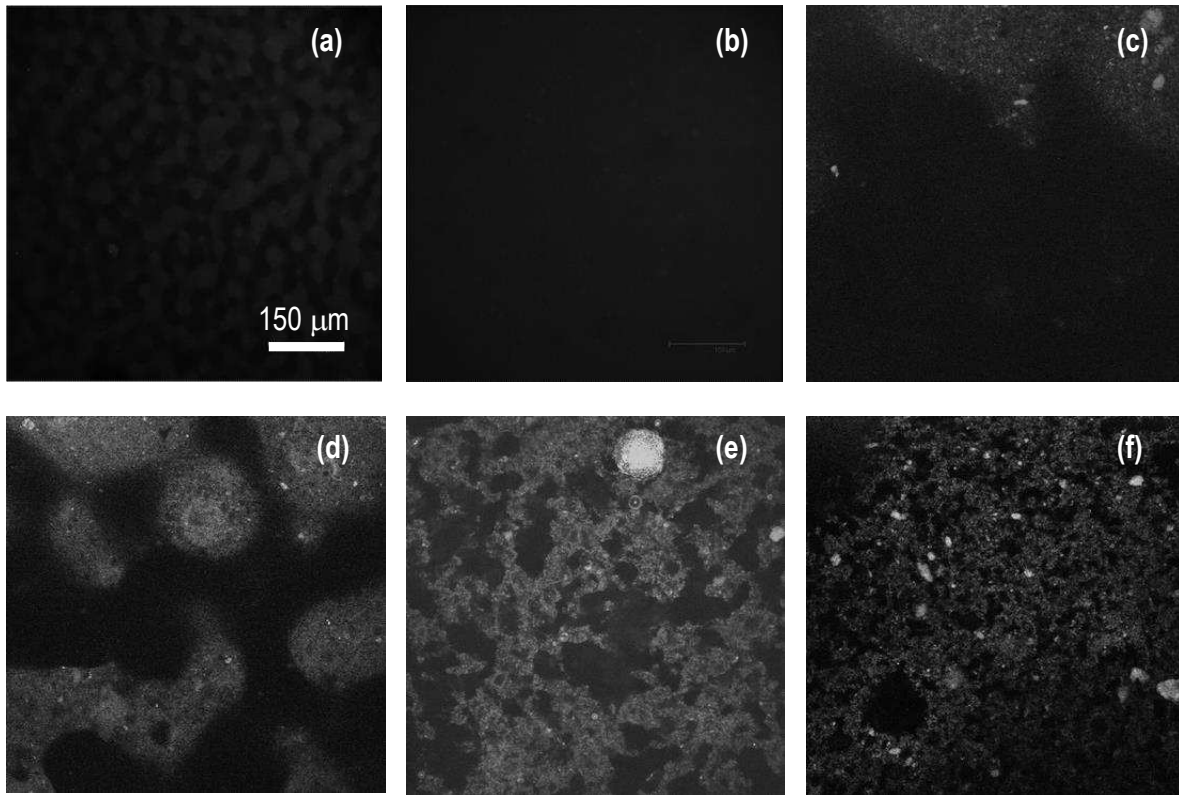
574

575

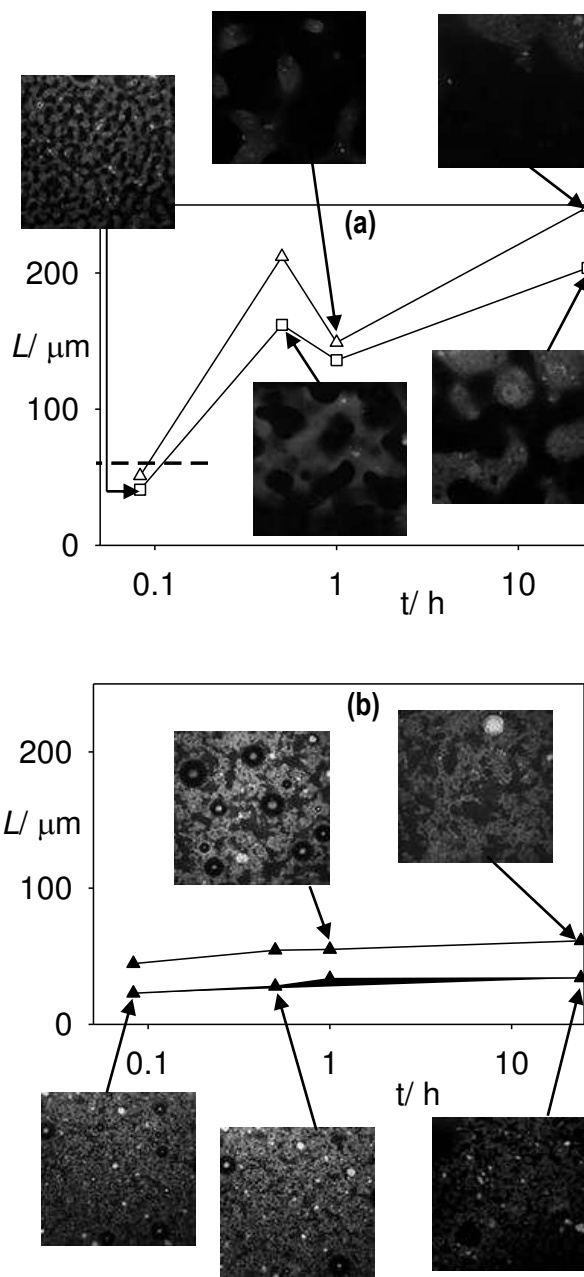
576 Figure 4



591 Figure 5
592
593
594

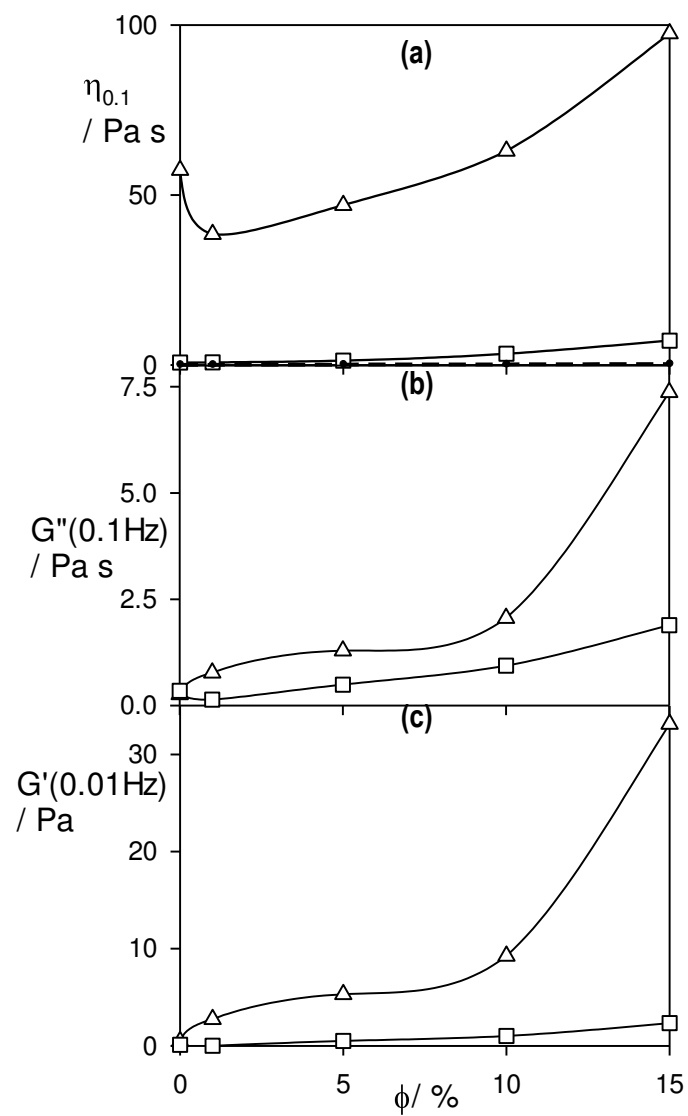


595 Figure 6
596
597



598 Figure 7

599



600

601

602

603 **Table 1.**

vol.%	K	n	P_K	P_m	R
pH 7					
1	0.022	0.96	<0.0001	0.37	0.3066
5	0.022	0.32	<0.0001	<0.0001	0.9823
10	0.037	0.48	<0.0001	<0.0001	0.9872
15	0.042	0.25	<0.0001	<0.0001	0.9973
pH 4					
1	0.019	0.37	<0.0001	<0.0001	0.9680
5	0.033	0.17	<0.0001	<0.0001	0.9982
10	0.0841	0.19	<0.0001	<0.0001	0.9934
15	6.96	-0.27	<0.0001	<0.0001	0.9985

604

605

606 **Figure & Table Captions**

607 **Fig.1.** Size distribution of WPI microgel particles. Intensity (I) versus particle size (d): before sonication
 608 (---); after sonication (—).

609 **Fig. 2.** CLSM micrographs of 5vol.% suspensions of WPI microgel particles at: (a) pH7; (b) pH4. Bright
 610 regions are WPI microgel particles, dark regions are background aqueous phase.

611 **Fig. 3.** Viscosity (η) versus shear rate ($d\gamma/dt$) for WPI microgel particle suspensions at: (a) pH 7; (b) pH
 612 4; for 1 vol.%(\circ, \bullet); 5 vol.%($\triangle, \blacktriangle$); 10 vol.%(\square, \blacksquare) and 15 vol.%(\diamond, \blacklozenge) particles. The curves show the
 613 fitted power law behaviour according to the parameters shown in Table 1.

614 **Fig. 4.** Appearance of W/W emulsions at 1, 3 and 7 days formed by mixtures containing 2 wt.% starch
 615 + 0.3 wt.% LBG, with 0 to 15 vol.% added WPI microgel particles at: (a) pH7; (b) pH 4.

616 **Fig.5.** Representative confocal micrographs of mixtures containing 2wt.% starch + 0.3 wt.% LBG in the
 617 absence and presence WPI microgel particles: (a) no particles, age 5min; (b) no particles, age 24 h; (c)
 618 5 vol.% WPI particles, pH 7, age 24 h; (d) 10 vol.% WPI particles, pH 7, age 24 h; (e) 5 vol.% WPI
 619 particles, pH4, age 24 h; (f) 10 vol.% WPI particles, pH4, age 24 h

620 **Fig.6.** Characteristic length scale, L , versus time since mixing for 2 wt.% starch + 0.3 wt.% LBG at:(a)
 621 pH 7; (b) pH 4; for 5 vol.% (\triangle) and 10 vol.% (\square) added WPI microgel particles. Representative
 622 micrographs are shown for various systems and times as indicated by the arrows. The dashed line
 623 shows $L \approx 60 \mu\text{m}$ after 5min the absence of particles.

624 **Fig.7(a)** Viscosity at shear rate 0.1 s^{-1} ; ($\eta_{0.1}$); (b) storage modulus (G') measured at 0.1 Hz and 0.01
 625 strain; (G'') loss modulus measured at 0.1 Hz and 0.01 strain: versus vol.%(ϕ) of WPI microgel particles
 626 at pH 4 added to individual solutions of: 4 wt.% starch (\triangle); 0.6 wt.% LBG(\square).

627 **Table 1.** Fitting parameters of power law model (eq. 1) to viscosity of WPI microgel suspensions of
 628 different concentrations(vol.%), as shown in Figure 3. P_K and P_m are P values for fitted K and n values,
 629 respectively, and R is the global goodness of fit.

630

631